Excitations in a quantum spin liquid with random bonds

D. Hüvonen,[1] S. Zhao,[1,*] G. Ehlers,[2] M. Månsson,[1] S. N. Gvasaliya,[1] and A. Zheludev[1,†]
[1]*Neutron Scattering and Magnetism, Laboratory for Solid State Physics, ETH Zurich, 8006 Zurich, Switzerland*
[2]*Oak Ridge National Laboratory, Oak Ridge, Tennessee 37831, USA*
(Received 23 October 2012; published 10 December 2012)

We present the results of an inelastic neutron-scattering study on two bond disordered quasi-two-dimensional quantum magnets $(C_4H_{12}N_2)Cu_2(Cl_{1-x}Br_x)_6$ with $x = 0.035$ and 0.075. We observe an increase of spin gap, a reduction of magnon bandwidth, and a decrease of magnon lifetimes compared to the $x = 0$ sample. Additional magnon damping is observed at higher energies away from the zone center, which is found to follow the density of single-particle states.

DOI: 10.1103/PhysRevB.86.214408 PACS number(s): 75.10.Kt, 75.30.Ds, 74.62.En, 72.10.Di

I. INTRODUCTION

Disordered quantum magnets are expected to exhibit qualitatively different behavior from pure systems. Apart from straightforward chemical substitution of the magnetic ions for nonmagnetic counterparts, a more recently implemented idea focuses on creating disorder on peripheral sites involved in superexchange interactions.[1–5] Theoretical predictions and scarce experimental work dealing with stability of spin gap,[6] lifetime of excitations,[7,8] appearance of in-gap localized states,[9,10] and novel quantum phases[11] in the presence of disorder necessitate further experiments. In the current paper we discuss the impact of random bond disorder on spin dynamics in a quasi-two-dimensional gapped quantum magnet as seen by inelastic neutron-scattering experiments. Our choice of parent compound is a well-characterized Heisenberg quantum magnet piperazinium hexachlorodicuprate (PHCC).[12–14] It features a layered structure with a complex spin network of $S = 1/2$ Cu^{2+} ions bridged by Cu-Cl-Cl-Cu superexchange pathways (see Fig. 1). The ground state is a nonmagnetic spin liquid, and the low-energy excitation spectrum consists of a sharp magnon mode with a gap of $\Delta = 1$ meV and bandwidth of about 1.7 meV. Considerable attention has been devoted to magnon lifetimes in PHCC due to observed single magnon decay into two magnons as the two energy scales meet.[15–17] Our focus is on determining the magnon spectrum, its temperature dependence, and magnon lifetimes in bond disordered PHCC derivatives. We find that, although no drastic modification of the spectrum occurs, bond disorder increases spin gap and reduces magnon bandwidth and lifetime. A random-phase approximation (RPA) treatment of an effective dimer model accounts for the temperature induced blueshift of the gap and the drop of intensity in this complex material. The most notable effect of bond disorder is the increase of magnon lifetimes, which can be correlated with the single magnon density of states function.

II. SAMPLES AND EXPERIMENTAL METHODS

PHCC crystallizes in a triclinic $P\bar{1}$ group with lattice parameters $a = 7.9691(5)$ Å, $b = 7.0348(5)$ Å, and $c = 6.0836(4)$ Å and angles $\alpha = 111.083(3)^\circ$, $\beta = 99.947(3)^\circ$, and $\gamma = 81.287(4)^\circ$. Bond disordered PHCC samples with 3.5 and 7.5% nominal Br content (referred to as PHCX) were prepared by adjusting the HCl:HBr solvent ratio in the starting solutions. Large fully deuterated single crystals were grown by the thermal gradient method.[18] Samples used in the inelastic neutron-scattering experiments were mosaics of three crystals coaligned to within half a degree with total masses of 3.21 and 4.27 g for the 3.5 and the 7.5% Br samples, respectively. Lattice parameters at 1.6 K were $a = 7.86$ Å, $b = 6.96$ Å, $c = 6.08$ Å, and angles $\alpha = 111.23^\circ$, $\beta = 99.95^\circ$, and $\gamma = 81.26^\circ$ for the 3.5% Br sample and $a = 7.90$ Å, $b = 6.97$ Å, $c = 6.03$ Å, and angles $\alpha = 111.15^\circ$, $\beta = 99.91^\circ$, and $\gamma = 81.29^\circ$ for the 7.5% Br sample. Time-of-flight (TOF) neutron-scattering experiments were carried out on the direct scattering geometry CNCS instrument[19] at Spallation Neutron Source in Oak Ridge National Laboratory with 4.2-meV incident energy neutrons. Triple axis neutron spectroscopy measurements were performed on the TASP instrument at Paul Scherrer Institute.[20] At TASP two modes of operation were used, which we denote as the high-resolution and the low-resolution mode. In low-resolution mode a fixed 5-meV final energy and detector distance of 75 cm with slit width of 30 mm were used. In high-resolution mode a fixed 3.5-meV final energy was used and the detector analyzer distance was increased to 90 cm along with narrowing the slit to 20 mm in front of the detector. A collimator of 80 minutes was placed after the monochromator and a liquid nitrogen cooled Be filter was employed between the sample and the analyzer at all times. The resolutions as determined from the incoherent elastic scattering line widths at half maximum were 0.10 meV in high-resolution mode and 0.25 meV in low-resolution mode. The sample environment was a standard Orange cryostat in all experiments.

III. RESULTS

The low-energy excitation spectrum up to 3 meV was recorded by making full 360° rotations with a 1° step at CNCS for the 3.5 and 7.5% Br samples. Using the scattering plane determined by (1,0,0) and $(0,1,\bar{1})$ reciprocal-lattice vectors the 190° horizontal and 32° vertical acceptance angles of the detector bank allowed probing of several Brillouin zones simultaneously (Fig. 1). Recorded events were projected to the reciprocal sample coordinate system and binned into a four-dimensional (H,K,L,E) matrix of size $101 \times 101 \times 101 \times 96$ spanning from $(-3.5,-2.5,-2.5,-0.5)$ to (3.5,2.5,2.5,3.3) using the MANTID[21] program. Two-dimensional projections from the full spectrum along the three main reciprocal

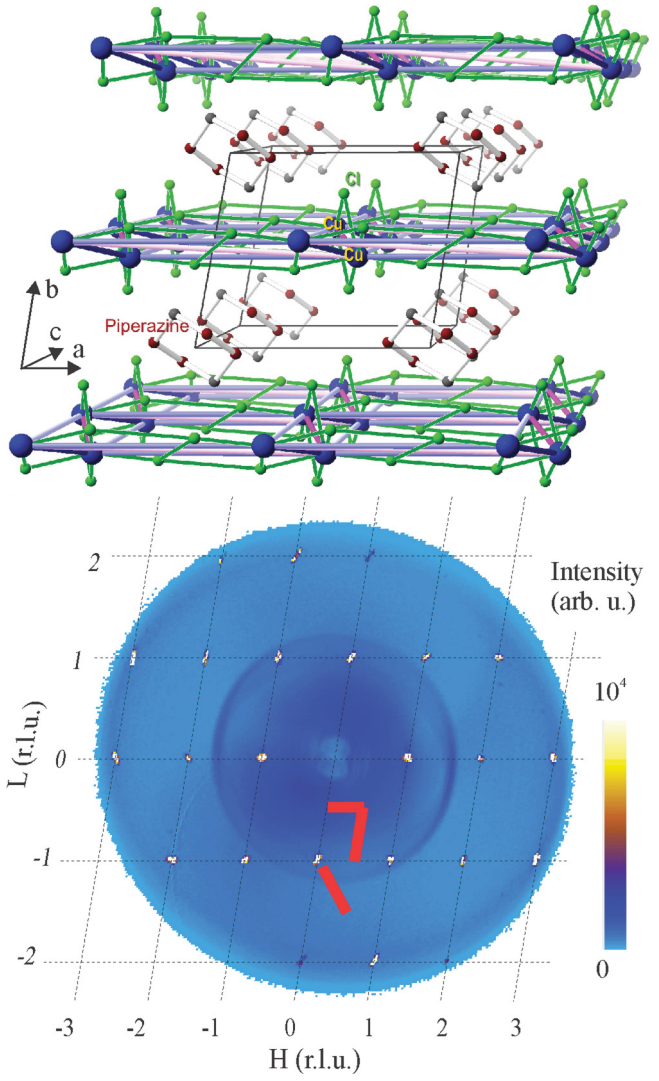

FIG. 1. (Color online) Top: Structure of PHCC; magnetic Cu^{2+} (blue) ions are coupled via Cl (green) ions to form 2D layers separated by piperazine molecules; thick lines within layers indicate possible superexchange pathways. Bottom: Elastic neutron-scattering intensity in the (H,L) plane (integrated over the K direction) in the 3.5% Br sample showing the TOF experiment detector coverage; thick red lines show the locations of the triple axis scans projected onto the (H,L) plane.

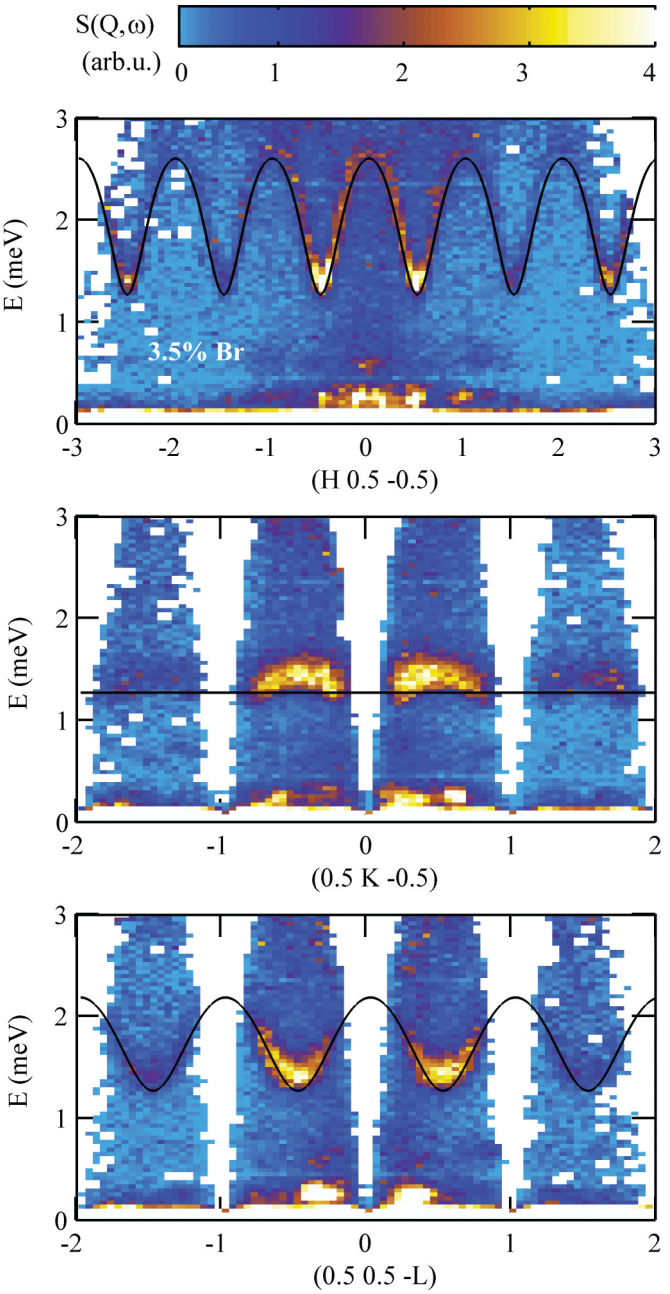

FIG. 2. (Color online) False color intensity maps of the dynamic structure factor $S(\mathbf{Q},\omega)$ of the 3.5% Br PHCX sample along the three main reciprocal-lattice directions. The constant reciprocal coordinates denote center points of integration ranges over ± 0.1 reciprocal lattice units. Data from distant unit cells have been backfolded to the first Brillouin zone. Note that some spurious scattering from instrumental origin is visible at wave vectors close to the direct beam. The solid lines are the fitted dispersion curves from triple axis data, Eq. (1) and Table I.

directions are shown in Figs. 2 and 3. In these figures $S(\mathbf{Q},\omega)$ along the constant reciprocal coordinates was integrated over the ± 0.1 range and backfolded to the first Brillouin zone. A dispersive gapped magnon mode is clearly visible in both samples. It is evident that no drastic modifications to the excitation spectrum occur in the bond disordered samples. Note that in the chosen sample orientation and instrument configuration we were unable to probe $K = -L \approx 0$ and the equivalent parts spectrum for $E \geqslant 0.3$ meV.

The magnon linewidth and its wave-vector dependence were studied in greater detail by triple axis spectroscopy in conjunction with the well-established resolution calculation methods using Popovici approximations[22] embedded in the RESLIB package. Constant-Q scans at the zone center measured in high-resolution mode of TASP at a temperature of 1.6 K were already shown in Fig. 4 of Ref. 3. As noted previously the intrinsic magnon linewidth and the resonance energy are considerably increased with bond disorder. Although it is known from recent electron-spin resonance studies[23,24] that the magnon band is split by 0.038 meV due to anisotropy, this splitting is small enough compared with our experimental resolution to justify the use of single mode approximation.

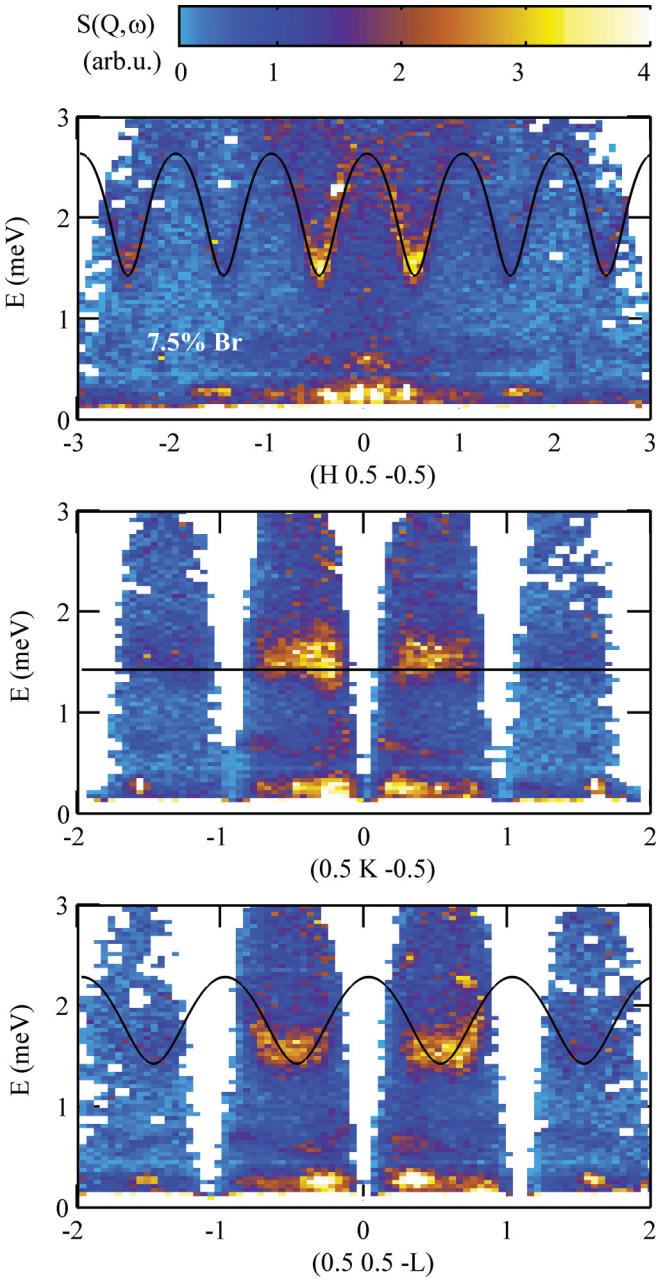

FIG. 3. (Color online) False color intensity maps of the dynamic structure factor $S(\mathbf{Q},\omega)$ of the 7.5% Br PHCX sample along the three main reciprocal-lattice directions. Coordinates and lines are as in Fig. 2.

Moreover, it has been established that for the 10% Br sample the splitting is reduced by a factor of 2.[25] Hence, broadening is a lifetime effect induced by disorder.

Temperature evolution of the magnon at the zone center was studied on TASP using low-resolution mode for the broader resonance of the 7.5% Br sample and using high-resolution mode for the 3.5% Br sample. Constant-Q scans across magnon energy at different temperatures are shown in Fig. 4. Blueshift and damping with increasing temperature are evident for both samples.

Triple axis spectroscopy was used to study the magnon wave-vector dependence in the low-resolution mode at

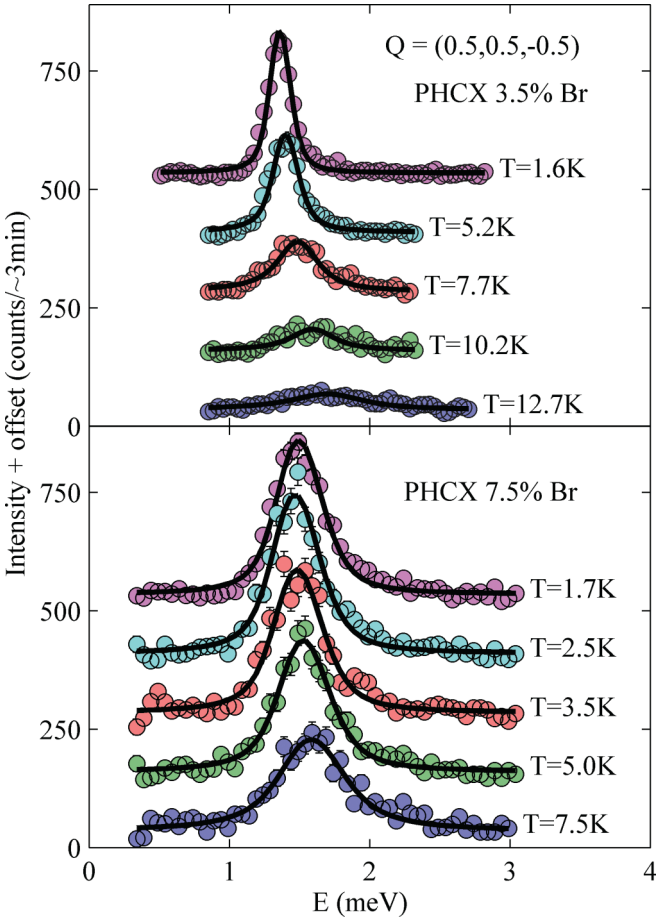

FIG. 4. (Color online) Constant-Q scans across the magnon energy at different temperatures for the 3.5 and 7.5% Br samples. Corresponding solid lines are fitted Lorentzian energy profiles convoluted with the four-dimensional instrumental resolution function.

$T = 1.6$ K. Measured spectra at different wave vectors were iteratively fitted with resolution convoluted Lorentzian line shapes while adjusting the parameters in the dispersion relation (Figs. 5 and 6). Following the in-depth analysis of unperturbed PHCC[13] we parametrized the magnon dispersion:

$$\hbar\omega(\mathbf{Q}) = (B_0 + \gamma_{\mathbf{Q}})^{\frac{1}{2}},$$
$$\gamma_{\mathbf{Q}} = B_h \cos(2\pi h) + B_l \cos(2\pi l) + B_{hl}\{\cos[2\pi(h+l)] + \cos[2\pi(h-l)]\} + B_{2h}\cos(4\pi h) + B_{2l}\cos(4\pi l). \quad (1)$$

Best fitting parameters are collected in Table I for comparison. Fitted wave-vector-dependent magnon energies and linewidths are shown as symbols in Fig. 7. Key observations are that at $Q = (0.5,0.5,-0.5)$ the gap increases from 1 meV to 1.36 and 1.50 meV for the 3.5 and the 7.5% Br samples, respectively. At the same time the bandwidth is reduced by about 0.2 meV from 1.74 meV to 1.53 and 1.58 meV.

The bandwidth reduction is likely a consequence of modification of averaged exchange constants due to induced chemical pressure by Br substitution. In addition we observed that the magnon damping rate increases notably (by approximately a

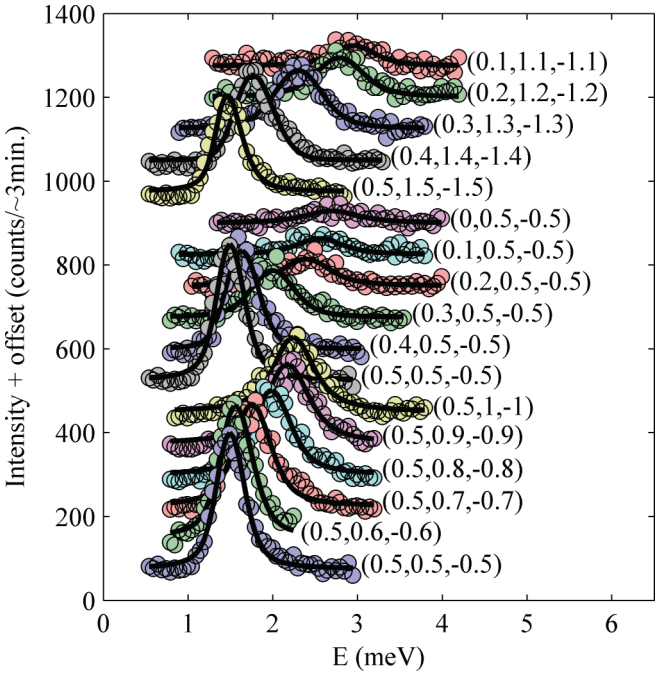

FIG. 5. (Color online) Constant-Q scans across the magnon energy at different wave vectors (shown in parentheses) for the 7.5% Br sample. Corresponding solid lines are the fitted Lorentzian energy profiles convoluted with the four-dimensional instrumental resolution function.

factor of 3) when moving toward zone boundaries. This drastic shortening of the magnon lifetimes will be discussed in the next section.

Note that there exists a small dispersion perpendicular to magnetic layers as seen from TOF spectra (middle panels of Figs. 2 and 3). However, in our fitting of the dispersion relation parameters using triple axis spectroscopy data the used sample orientation did not allow us to extract the magnitude of the interlayer coupling independently, and hence we fixed it to zero as was done for the case of unperturbed PHCC.[13] The smallness of the interlayer coupling and the fact that the sample orientation was not optimized to measure dispersion along the (0,1,0) direction do not allow us to make a quantitative estimate of the value from current experimental results. A small interlayer coupling can renormalize exact spin gap and bandwidth values slightly but the conclusions on the disorder effect remain qualitatively intact.

IV. DISCUSSION

Random-phase approximation (RPA) has been successful in describing the dispersion of crystal-field excitations in several rare-earth compounds,[26] as well as magnon dispersion in several dimerized transition-metal-based magnets.[27–30] Even though the exact microscopic Hamiltonian remains unknown for PHCC and satisfactory coincidence with the experimental spectrum has been obtained considering several magnetic Hamiltonians[13,31] the formal description of the spectrum [Eq. (1)] is valid for RPA treatment. Namely, the gap is introduced by an effective dimer coupling $J_0 = \sqrt{B_0}$ and the rest of the spectrum is dominated by smaller magnetic couplings $B_{n(h,l)}$. Hence, we can write for the temperature

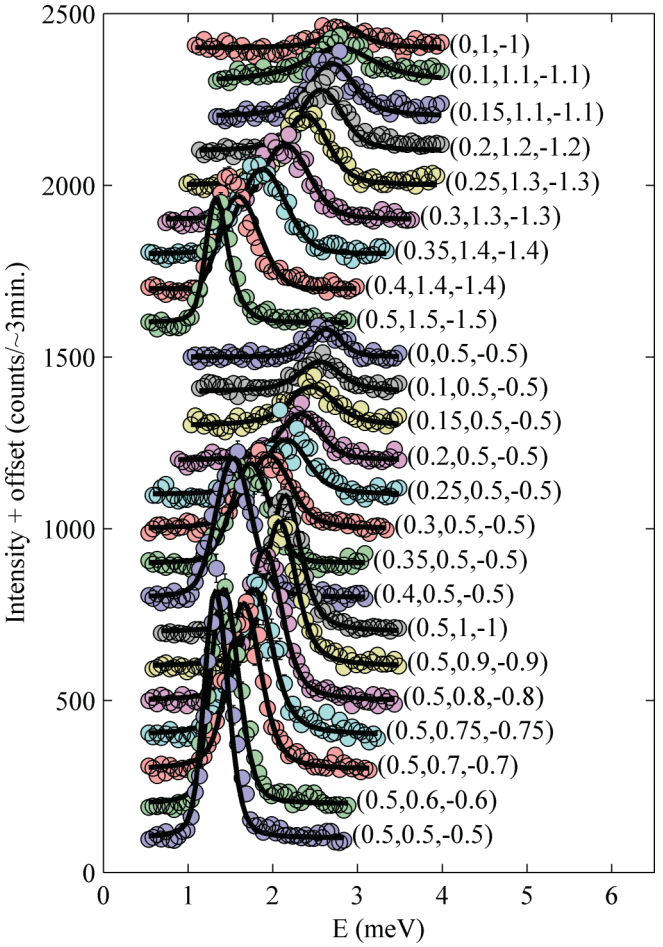

FIG. 6. (Color online) Constant-Q scans across the magnon energy at different wave vectors (shown in parentheses) for the 3.5% Br sample. Corresponding solid lines are fitted Lorentzian energy profiles convoluted with the four-dimensional instrumental resolution function.

renormalized gap[27] $\hbar\omega(T)_{\mathbf{Q}} = (B_0 + R(T)\gamma_{\mathbf{Q}})^{\frac{1}{2}}$. Here $R(T)$ is the population difference of the singlet ground state and the triply degenerate first excited state $R(T) = n_S - n_T = (1 - e^{-\beta J_0})/(1 + 3e^{-\beta J_0})$. The intensity of the excitation is directly proportional to the population difference of the ground and the excited states. Taking the intensity of the magnon peak at low temperature as a scaling constant we expect $I(T)/I(1.6K) = R(T)$. Finite temperature renormalization of the magnon energy and intensity at the dispersion minimum are

TABLE I. Best fit parameters to describe magnon dispersion by Eq. (1) for 3.5% Br and 7.5% Br PHCX samples in comparison with PHCC from Ref. 13

Parameter (meV^2)	0% Br [13]	3.5% Br	7.5% Br
B_0	5.44(2)	5.50(4)	6.12(7)
B_h	2.06(3)	2.17(5)	2.34(9)
B_l	1.07(3)	1.02(5)	1.28(8)
B_{hl}	−0.39(1)	−0.20(2)	−0.05(4)
B_{2h}	−0.34(3)	−0.15(4)	−0.19(7)
B_{2l}	−0.22(2)	0.00(4)	−0.04(6)

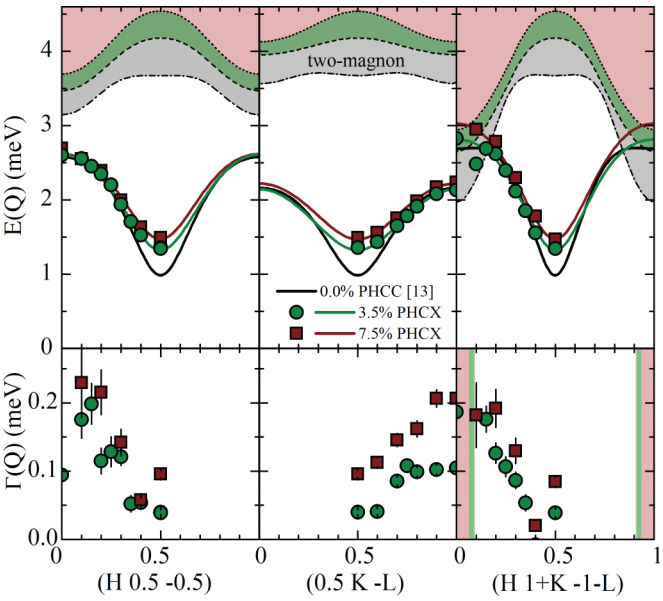

FIG. 7. (Color online) Magnon excitation energies at 1.6 K and the corresponding linewidths shown with green circles and red squares for the 3.5 and 7.5% Br samples, respectively, along the three reciprocal space directions. Solid lines are the fitted dispersion curves described by Eq. (1) with the parameters listed in Table I. Shaded areas bounded by dotted, dashed, and dash-dotted lines represent two magnon continua for the 7.5, 3.5 and 0% Br samples, respectively.

shown in Fig. 8. We see that for all the samples the temperature induced blueshift and the intensity drop are explained by a RPA treatment of an effective dimer model without any adjustable parameters. Temperature dependence of the magnon linewidths will be discussed in detail elsewhere.[24]

As a result of bond disorder the long lived magnon excitations get notably damped. Damping rate is smallest at the zone center $Q = (0.5,0.5,-0.5)$ and increases by about a factor of 3 at zone boundaries for all measured directions. This is in contrast to unperturbed PHCC, where significant damping occurs only at wave vectors where the two magnon continuum has a minimum below the single magnon

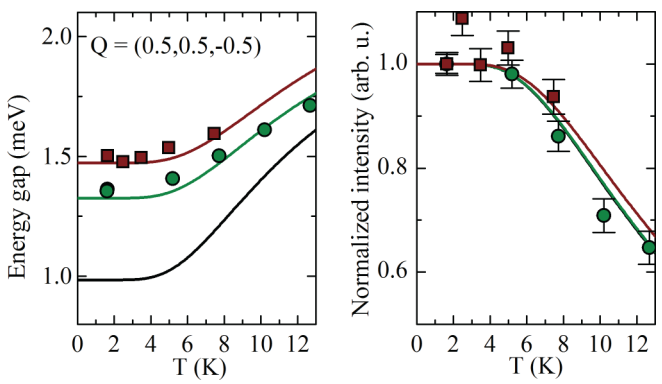

FIG. 8. (Color online) Left: Gap renormalization as a function of temperature: green circles and red squares are magnon energies at $Q = (0.5,0.5,-0.5)$ for the 3.5 and 7.5% Br samples; solid lines are the RPA predictions. Right: Intensity of the magnon peak normalized to 1.6-K intensity; lines are population differences of the singlet and triplet states (see discussion in text).

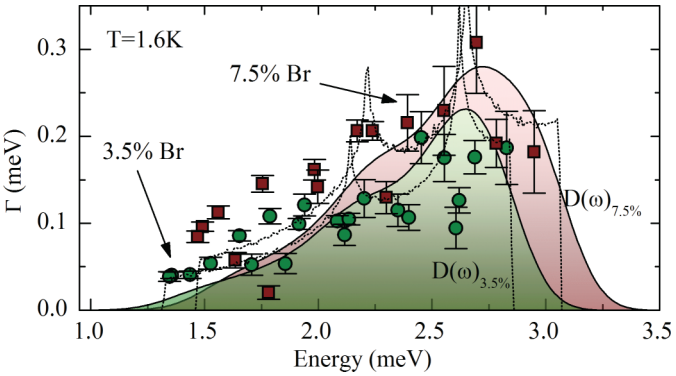

FIG. 9. (Color online) Intrinsic magnon linewidths for the 3.5% Br (green circles) and 7.5% Br (red squares) PHCX samples collected from Fig. 7. Dash-dotted lines are the corresponding scaled densities of magnon states. Solid envelopes are the corresponding resolution convoluted densities of state.

spectrum.[32] A similar albeit less rapid increase of damping rates with the wave vector has been reported in Haldane spin chain compound $CsNiCl_3$[33] as opposed to IPA-$CuCl_3$, where the single quasiparticle spectrum terminates altogether at the point of the crossing.[34] Using the experimentally determined magnon dispersion relation, Eq. (1), we calculate the energy of the lower boundary of the two magnon continuum $\hbar\omega_{2L}(\mathbf{Q}) = \min[\hbar\omega(\mathbf{Q_1}) + \hbar\omega(\mathbf{Q_2})]|_{\mathbf{Q_2}=\mathbf{Q}-\mathbf{Q_1}}$ and plot it as envelopes of the shaded areas in Fig. 7. As a direct consequence of the bandwidth reduction in the PHCX samples the two magnon continuum drops below the single-particle spectrum only in a very narrow wave-vector range (see the shaded areas in the bottom right panel of Fig. 7). Hence, we can conclude that the two-particle decay cannot account for the observed lifetime reduction in PHCX samples.

On the other hand, in bond disordered samples the magnons can scatter off impurities. Assuming that this process is elastic, the available final state is a magnon with the same energy. In this case the scattering rate would follow the density of single magnon states (DOS) at particular energy $\Gamma(\omega) \propto D(\omega)$. To test this assumption we calculated $D(\omega)$ numerically for both PHCX samples by discretizing the spectrum described by Eq. (1) and convoluted it with the experimental energy resolution of the inelastic neutron experiment. These DOS curves are shown with solid line envelopes in Fig. 9. The comparison gives remarkably good qualitative agreement. This result highlights the difference between disorder and temperature induced magnon lifetime shortening. In a disorder-free system magnon lifetimes shorten due to mutual collisions. However, in these collisional processes the energy of a single magnon need not be conserved and a qualitatively different set of two magnon final states is allowed.[30,35,36]

V. CONCLUSIONS

We have measured the excitation spectrum up to 4 meV of two bond disordered quasi-two-dimensional quantum magnets. No localized states were found to appear within the spin gap, and the excitation spectrum remains qualitatively similar to that of the unperturbed material. However, the spin gap increases and a reduction of bandwidth occurs. We attribute these

effects to chemical pressure induced by Br substitution, which affects the superexchange strengths. For both 3.5 and 7.5% Br samples RPA explains the temperature induced blueshift of the magnon mode at the zone center. The drop of the magnon peak intensity with temperature is consistent with a singlet-triplet population difference of an effective dimer model. The long lived quasiparticles of the parent compound acquire finite lifetimes with damping rate increasing away from the zone center in all directions. The damping rate in disordered samples follows the density of single magnon states.

ACKNOWLEDGMENTS

This work is partially supported by the Swiss National Fund under Project No. 2-77060-11 and through Project 6 of MANEP. Research at Oak Ridge National Laboratory's Spallation Neutron Source was supported by the Scientific User Facilities Division, Office of Basic Energy Sciences, US Department of Energy. We thank T. Yankova and Dr. V. Glazkov for their involvement in the early stages of this project.

*Current address: FBS Swiss Federal Institute of Technology (EPFL), CH-1015 Lausanne, Switzerland.

†http://www.neutron.ethz.ch/

[1]T. Hong, A. Zheludev, H. Manaka, and L.-P. Regnault, Phys. Rev. B **81**, 060410 (2010).

[2]E. Wulf, S. Mühlbauer, T. Yankova, and A. Zheludev, Phys. Rev. B **84**, 174414 (2011).

[3]D. Hüvonen, S. Zhao, M. Månsson, T. Yankova, E. Ressouche, C. Niedermayer, M. Laver, S. N. Gvasaliya, and A. Zheludev, Phys. Rev. B **85**, 100410(R) (2012).

[4]F. Yamada, H. Tanaka, T. Ono, and H. Nojiri, Phys. Rev. B **83**, 020409 (2011).

[5]R. Yu, L. Yin, N. S. Sullivan, J. S. Xia, C. Huan, A. Paduan-Filho, N. F. Oliveira, Jr., S. Haas, A. Steppke, C. F. Miclea, F. Weickert, R. Movshovich, E.-D. Mun, B. L. Scott, V. S. Zapf, and T. Roscilde, Nature **489**, 379 (2012).

[6]R. A. Hyman, K. Yang, R. N. Bhatt, and S. M. Girvin, Phys. Rev. Lett. **76**, 839 (1996).

[7]L. P. Regnault, J. P. Renard, G. Dhalenne, and A. Revcolewchi, Europhys. Lett. **32**, 579 (1995).

[8]G. Xu, C. Broholm, Y.-A. Soh, G. Aeppli, J. F. DiTusa, Y. Chen, M. Kenzelmann, C. D. Frost, T. Ito, K. Oka, and H. Takagi, Science **317**, 1049 (2007).

[9]E. S. Sørensen and I. Affleck, Phys. Rev. B **51**, 16115 (1995).

[10]W. Wang, S. Qin, Z. Y. Lu, L. Yu, and Z. Su, Phys. Rev. B **53**, 40 (1996).

[11]M. P. A. Fisher, P. B. Weichman, G. Grinstein, and D. S. Fisher, Phys. Rev. B **40**, 546 (1989).

[12]A. Daoud, A. B. Salah, C. Chappert, J. P. Renard, A. Cheikhrouhou, T. Duc, and M. Verdaguer, Phys. Rev. B **33**, 6253 (1986).

[13]M. B. Stone, I. Zaliznyak, D. H. Reich, and C. Broholm, Phys. Rev. B **64**, 144405 (2001).

[14]M. B. Stone, C. Broholm, D. H. Reich, P. Schiffer, O. Tchernyshyov, P. Vorderwisch, and N. Harrison, New J. Phys. **9**, 31 (2007).

[15]M. B. Stone, C. Broholm, D. H. Reich, O. Tchernyshyov, P. Vorderwisch, and N. Harrison, Phys. Rev. Lett. **96**, 257203 (2006).

[16]A. Kolezhuk and S. Sachdev, Phys. Rev. Lett. **96**, 087203 (2006).

[17]M. E. Zhitomirsky and A. L. Chernyshev, arXiv:1205.5278.

[18]T. Yankova, D. Hüvonen, S. Mühlbauer, D. Schmidiger, E. Wulf, S. Zhao, A. Zheludev, T. Hong, V. O. Garlea, R. Custelcean, and G. Ehlers, Philos. Mag. **92**, 2629 (2012).

[19]G. Ehlers, A. A. Podlesnyak, J. L. Niedziela, E. B. Iverson, and P. E. Sokol, Rev. Sci. Instrum. **82**, 085108 (2011).

[20]F. Semadeni, B. Roessli, and P. Boni, Physica B **297**, 152 (2001).

[21]http://www.mantidproject.org

[22]M. Popovici, Acta Crystallogr. A **31**, 507 (1975).

[23]V. N. Glazkov, T. S. Yankova, J. Sichelschmidt, D. Hüvonen, and A. Zheludev, Phys. Rev. B **85**, 054415 (2012).

[24]B. Nafradi (unpublished).

[25]V. Glazkov (private communication).

[26]J. Jensen and A. R. Mackintosh, *Rare Earth Magnetism: Structures and Excitations* (Clarendon, Oxford, 1991).

[27]B. Leuenberger, A. Stebler, H. U. Güdel, A. Furrer, R. Feile, and J. K. Kjems, Phys. Rev. B **30**, 6300 (1984).

[28]Y. Sasago, K. Uchinokura, A. Zheludev, and G. Shirane, Phys. Rev. B **55**, 8357 (1997).

[29]A. Zheludev, J. M. Tranquada, T. Vogt, and D. J. Buttrey, Phys. Rev. B **54**, 6437 (1996).

[30]N. Cavadini, C. Rüegg, W. Henggeler, A. Furrer, H. G. Güdel, K. Kramer, and H. Mutka, Eur. Phys. J. B **18**, 565 (2000).

[31]H.-J. Mikeska and M. Müller, Appl. Phys. A **74**, S580 (2002).

[32]M. B. Stone, I. A. Zaliznyak, T. Hong, C. L. Broholm, and D. H. Reich, Nature (London) **440**, 187 (2006).

[33]I. A. Zaliznyak, S.-H. Lee, and S. V. Petrov, Phys. Rev. Lett. **87**, 017202 (2001).

[34]T. Masuda, A. Zheludev, H. Manaka, L.-P. Regnault, J.-H. Chung, and Y. Qiu, Phys. Rev. Lett. **96**, 047210 (2006).

[35]G. Xu, C. Broholm, D. H. Reich, and M. A. Adams, Phys. Rev. Lett. **84**, 4465 (2000).

[36]D. L. Quintero-Castro, B. Lake, A. T. M. N. Islam, E. M. Wheeler, C. Balz, M. Månsson, K. C. Rule, S. Gvasaliya, and A. Zheludev, arXiv:1208.5921.